BOND GRAPH APPROACH FOR MODELLING OF PROTON EXCHANGE MEMBRANE FUEL CELL SYSTEM

Kamyar Maleki Bagherabadi
PhD Candidate in Department of Marine Technology, Norwegian University of Science and Technology, Trondheim, NO-7491, Norway, kamyar.maleki@ntnu.no

Stian Skjong
Research Scientist in SINTEF Ocean, Trondheim, NO-7465, Norway, stian.skjong@sintef.no

Eilif Pedersen
Professor in Department of Marine Technology, Norwegian University of Science and Technology, Trondheim, NO-7491, Norway, eilif.pedersen@ntnu.no

ABSTRACT

The bond graph method proposes an approach for mathematical modeling of multi-domain systems by considering various energy conversions. This modeling theory is practical for predicting system behaviors besides investigating component operations with less computational time. Indeed, the modular view of the bond graph enables integration of sub-systems and components with logical graphical representation. Fuel cell systems as multi domains devices consist of auxiliary components and different physics such as pneumatic, electrochemical, electrical, thermodynamics and heat transfer. Providing proper models that can be utilized for investigating system performance with flexibility in configuration, integration, and size is desired point for developing studies. The bond graph method as a powerful multiphysics modeling tool facilitates fuel cell systems studies for further development of power systems in various applications. In this article, the PEMFC system with auxiliary components is modelled by the bond graph method.

Keywords: Polymer Exchange Membrane Fuel Cell System, Fuel Cell Modeling, Bond graph modelling, multi-domains system modeling

1 INTRODUCTION

Fuel cells directly produce electricity by chemical reactions between hydrogen and oxygen as reactants. These chemical reactions occur in the stack within the membrane. Fuel cells are also categorized based on electrolyte material, which determines the operational conditions of the system with specific temperature and pressure. Among the fuel cell types, the PEMFC with polymer electrolyte has a wide range of applications in transporting and stationary due to high efficiency, low operating temperature and fast start-up time. The PEMFC generates electricity by transferring protons among the membrane. The electrons travel from out circuit to produce electrical power in all fuel cell types. The Fuel cell performance depends on the auxiliary systems such as the air supply, the thermal management and the hydrogen supply (Pukrushpan, Stefanopoulou et al. 2004). The sub systems affect the over all efficiency and transient responses of the system.

Investigating the PEMFCs' behaviour as a component in power systems for various applications and conditions requires system level fidelity models. Therefore, a system level model for the fuel cells encompasses the sub-systems interactions to provide a practical prediction of the overall system performance. Moreover, fuel cell systems contain various domains and physics in the sub-systems. So, they are known as multi domains systems.

Fuel cells are usually modeled with three main modelling strategies regarding the fidelity and mathematical. High fidelity models are implemented with computational fluid dynamic (CFD) methods to investigate the stack behaviour precisely (Dawes, Hanspal et al. 2009). The CFD models can be used for designing and optimization of the membrane flow channels and chemical reactions with high computational efforts. However, Empirical models utilize correlations for the stack operational condition prediction with less computational time and usually the control volumes are assumed lumped (Chu, Jiang et al. 2000). Semi-empirical approaches consist of algebraic and ordinary differential equations for the system-level modeling purposes (Pukrushpan, Peng et al. 2004). The elecrochemical phenomenon are expressed by the empirical relations and mechanical sub-systems behaviour are captured by ordinary differential equations based on physics. The fuel cells system level models with real time capabilities are usually utilized to design the controllers or design optimizations applications. Hence, the computational time is an important parameter for using the models in simulators.

The bond graph as a multi disciplinary modeling strategy can be employed for the simulation of fuel cell systems with various sub-systems (Vijay, Samantaray et al. 2009). There are different energy conversions in fuel cell systems, which the bond graph capture them with power flow relations besides unified graphical representation. Indeed, the bond graph modular approach represents each sub-system individually and its connections to other components. The modelling approach provides estimation of the model behaviour with less computational time, which can be used for real time simulation applications (Benchouia, Elias et al. 2014).

This article presents the PEMFC model with system level fidelity by the bond graph approach. The main purpose is to present a modelling approach of the PEMFC system with the modular view of the sub-systems, which can be used for a wide range of applications. Because the PEMFCs have various power capacities, auxiliary system configurations and various application in stationary and transporting. This modular approach make the model flexible for further developments and adjustment with specific configurations. The PEMFC system is divided into sub-systems, which are modeled individually and connected through proper power conversion bonds. The model can be used for real time applications in simulators and adjusted to the specific PEMFC system power size and configuration.

2 FUEL CELL SYSTEM

The PEM fuel cell system as is shown in Figure 1 consists of a compressor and manifolds for the air supply, a hydrogen supply, a stack as the main section and a thermal management. The air is supplied by the compressor to the cathode and hydrogen is provided to the anode by a high pressure hydrogen tank. The chemical reactions are exothermic and the stack temperature increases. Therefore, the stack temperature is controlled by the external cooling system to maintain the system operation in high efficiency.

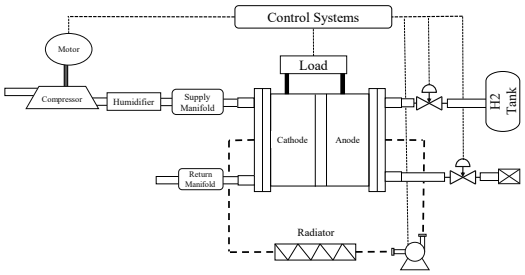

Figure 1: Schematic of the PEM fuel cell system

Among the auxiliary systems, the compressor consumes the most power, which affects the system efficiency. Also, the dynamics of filling the air manifolds determines the system response. So, the air supply system has a main role in the system efficiency and dynamic responses.

The main PEMFC system sections for modelling is shown in Figure 2 .The electrochemical stack operation depends on the air and hydrogen supplement. The gasses consumption and supplement rate determine the pressure and the temperature in the cathode and anode. Moreover, the electrochemical reactions heat dissipation in the stack and mass flows in the cathode and anode are considered in the thermal section.

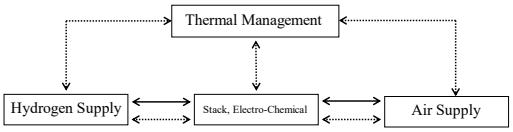

Figure 2: physical domains

3 FUEL CELL MODELLING

The PEMFC system is divided into sub-systems, which are modeled individually and connected with power conversions bonds. The main sub-system is the stack, the air supply, the hydrogen supply and the thermal management. The bond graph method is employed for modelling of this system. The bond graph consist of basic elements that are C (storage), I (induction), R(dissipation) and TF (transferring). These elements are connected with half arrow power bonds, which shows the power flow direction. Each bond consists of an effort and a flow. The causality of effort and flow are determined by a bar on the arrow. These bonds can be connected to the 0-junctions as summation of the flows or 1-junction as summation of the flows. The detailed explanation of the bond graph can be found in (Vasilyev, Andrews et al. 2017) .

3.1 Model assumptions

The model is based on the following assumptions:

- Gas dynamics are based on ideal gas relations and the thermal properties are independents of the temperature.
- The volumes are considered lumped.
- Gas transport friction has been neglected.
- The temperature is distributed uniformly along the cells, the stack and the cooling system.

3.2 Fuel Cell Stack Model

The heart of fuel cells is the stack as the schematic is shown in Figure 3. In the stack, hydrogen gas in the anodes is decomposed to positive ions, which transfer through electrolyte. The electrons pass the external circuit to satisfy the load (current). The transferred protons to the cathode produce water with the supplied oxygen from the air inlet. In the anode side, pure hydrogen gas is supplied and the outlet is usually dead ended. So, it is assumed that the whole provided hydrogen is consumed. The supplied air in the cathode consists of oxygen, nitrogen and water vapor. A portion of the oxygen supplied by the air sub-system is consumed and the water vapor is produced. Therefore, the partial pressures in the cathode are calculated in this model.

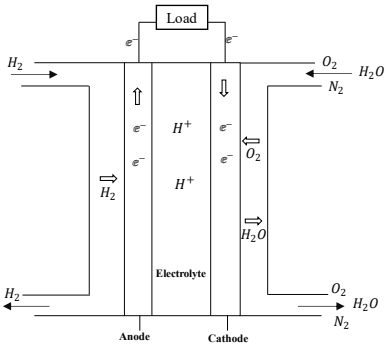

Figure 3: PEM stack

The stack voltage v_{st} is expressed by Equation 1, which consists of the reversible voltage E and electrical losses. The electrical losses are activation loss v_{act} , ohmic loss v_{ohm} and concentration loss v_{con}.

$$v_{st} = E - v_{act} - v_{ohm} - v_{con} \qquad 1$$

The reversible potential E^0 is determined by Equation 2 based on the Gibbs free energy ΔG and Faraday constant F.

$$E = E^0 - \frac{RT}{nF} ln\left[p^*_{H_2}\left(p^*_{O_2}\right)^{0.5}\right] \qquad 2$$

$$E^0 = -\frac{\Delta G}{2F}$$

The Gibbs free energy for each species hydrogen, oxygen and water is calculated by Equation with 3 chemical potentials μ_i, enthalpy Δh_i and entropy changes Δs_i. The bond graph schematic of this section is shown in Figure 4 .R is the gas constant, reference pressure $left(p_{ref} = 101325Pa\right)$ and temperature $T_{ref} = 298K$. The entropy s_i^0 and enthalpy h_i^0 for the reference condition are also summarized in Table 1.

$$\Delta G = \nu_{H_2}\mu_{H_2} + \nu_{O_2}\mu_{O_2} - \nu_{H_2O}\mu_{H_2O}$$
$$\mu_i = \Delta h_i - T\Delta s_i + RTlog\left(\frac{p_i}{p_{ref}}\right)$$
$$\Delta h_i = h_i^0\left(T - T_{ref}\right) \quad (3)$$
$$\Delta s_i = s_i^0 + M_i c_{pi} log\left(\frac{p_i}{p_{ref}}\right)$$

The produced heat from these chemical reactions $\dot{Q_{ch}}$ is calculated by Equation 4.

$$\dot{Q_{ch}} = -\Delta s_i T \dot{n_\iota} \quad (4)$$

Table 1: Reference entropy and enthalpy

Gas	$h^0([J/mol])$	$S^0[J/mol \cdot K]$
H_2	0	130.59
O_2	0	205.14
H_2O	-241820	188.83

3.2.1 Activation voltage

Portion of the reversible voltage is dedicated to initiate the chemical reactions in the anode and the cathode. This electrical loss is known as activation loss, which is considerable on the low currents. Activation loss occurs at the cathode surface and anode surface but is negligible at the anode side due to the fast reaction of hydrogen. The activation loss in this model is calculated by Equation 5 (Pukrushpan, Peng et al. 2004) .The cathode pressure p_{ca}, water vapor saturation pressure p_{sat} and the stack temperature T_{st} are main variables in the equation.

$$v_{act} = v_0 + v_a\left(1 - e^{-c_1 i}\right)$$
$$v_0 = 0.279 - 8.5 \times 10^{-4} \times (T_{st} - 298.15) + 4.3085 \times 10^{-5} T_{st} \quad (5)$$

$$v_a = -1.618 \times 10^{-5} T_{st} + 1.618 \times 10^{-2}\left(\frac{p_{O_2}}{0.1173} + p_{sat}\right)^2 + (1.8 \times 10^{-4} T_{st} - 0.166)\left(\frac{p_{O_2}}{0.1173} + p_{sat}\right) + (-5.8 \times 10^{-4} T_{st} + 0.5736) \quad (6)$$

Ohmic voltage

The protons transferring from the anode to the cathode through the membrane encounters a resistance that occurs in any substance as ohmic resistance. The ohmic resistance R_{ohm} is determined by Equation 7and dependent on the temperature, the pressure and mostly on the humidity of the membrane λ. The membrane thickness is $t_m = 0.00125$ m (Pukrushpan, Stefanopoulou et al. 2004).

$$v_{ohm} = i \cdot R_{ohm}$$
$$R_{ohm} = \frac{t_m}{\sigma_M} \quad (7)$$
$$\sigma_M = (b_{11}\lambda + b_{12}) exp\left(b_2\left(\frac{1}{303} - \frac{1}{T_{st}}\right)\right)$$

Concentration voltage

The diffusion layer provides the required amount of oxygen inside the cathode. In high loads, the consumed oxygen increases significantly. If the oxygen consumption rate overtakes the oxygen supply rate, a sharp voltage drop occurs. This voltage drop is due to lack of oxygen on the diffusion surface, which is known as concentration voltage. This electrical loss is expressed by Equation 8 (Pukrushpan, Stefanopoulou et al. 2004)The partial oxygen pressure p_{O_2} affects the electrical loss the most.

$$v_{conc} = i\left(c_2 \frac{i}{i_{max}}\right)^{c_3} \quad (8)$$

The electrical loss correlations are treated as algebraic equations and modeled with R components as shown in Figure 4 .The electrical losses are subtracted from reversible voltage and based on the energy conversion law are transferred as a heat flux to the thermal section.

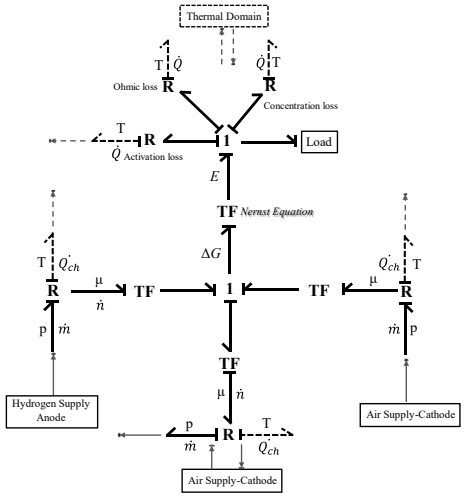

Figure 4: Electrochemical bond graph implementing

3.3 Air supply modeling

The air supply consists of the compressor, manifolds, and the cathode. This sub-system provides the required oxygen to the stack from supplying pressured air. The compressor consumes a significant amount of power compared to other auxiliary components. In addition, the inertia of the compressor and air filling of the manifolds and the cathode determine the system transient responses. Therefore, the consumed power by the compressor is considered in the system efficiency and dynamics.

The air supply bond graph implemented as shown in Figure 5. The compressor is controlled by a voltage signal and the pressure and mass flow rate relations are based on a real compressor map (Pukrushpan, Stefanopoulou et al. 2004).

The compressor motor torque τ_{cm}, the mass flow rate $\dot{m_{cp}}$ and the air pressure are obtained by Equation 9. The compressor electrical constant parameters are given in Table 2 (Pukrushpan, Stefanopoulou et al. 2004).

$$\tau_{cm} = \eta_{cm} \frac{k_t}{R_c m} \left(v_{cm} - k_v \omega_{cp}\right) \qquad 9$$

$$J_{cp} \frac{d\omega_{cp}}{dt} = \tau_{cm} - \tau_{cp} \left[\left(\frac{p_{sm}}{p_{atm}} \right)^{\frac{\gamma-1}{\gamma}} - 1 \right] \dot{m_{cp}}$$

The pressure in the C elements as reservoir of energy and mass are determined by the ideal gas relation in Equation 10. The gas dynamics are modelled by the pseudo bond graphs (Karnopp 1978) (Pedersen 2001).

$$\frac{dp}{dt} = \frac{R_a T}{V} (\dot{m_{in}} - \dot{m_{out}}) \qquad 10$$

The mass flow rate in the cathode inlet valve due to less pressure difference is estimated linearly by Equation 11.

$$\dot{m_{sm}} = k_{Ca_{in}} (p_{sm} - p_{ca}) \qquad 11$$

The cathode pressure p_{ca} is summation of the partial pressures of oxygen p_{O_2}, nitrogen p_{N_2} and water vapor p_{H_2O} as shown in Equation 12.

$$p_{ca} = p_{O_2} + p_{N_2} + p_{H_2O} \qquad 12$$

The pressure in the return manifold is calculated by Equation 13, which is implemented by a C element.

$$\frac{dp_{rm}}{dt} = \frac{R_a T_{rm}}{v_{rm}} \left(\dot{m_{ca,out}} - \dot{m_{rm,out}}\right) \qquad 13$$

The mass flow rate in the return manifold due to high pressure difference is estimated by non-linear that can be found in the reference(Pukrushpan, Stefanopoulou et al. 2004).

Table 2: Compressor parameters

$Item$	Description	Unit	Value
γ	Air ratio specific heat	-	1.4
C_p	Air specific heat in constant pressure	$j \cdot kg^{-1} \cdot K^{-1}$	350

k_v	Motor constant	$V/(rad/s)$	0.0153
k_t	Motor constant	$N - m/amp$	0.0153
J_{cp}	Compressor and motor inertia	$kg \cdot m^2$	5×10^{-5}

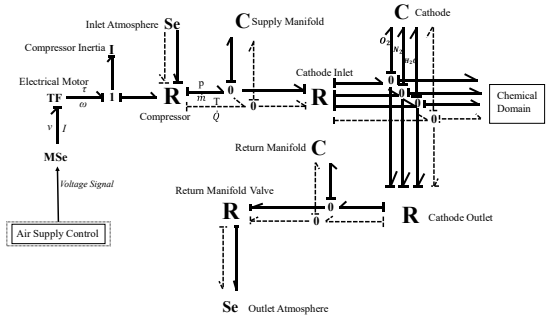

Figure 5 : Air supply implemented by bond graph

3.4 Thermal management and cooling system

The PEMFC has a specific temperature operating range of ($60 - 80 \circ C$),which due to safety and efficient operation should be maintained in this range. The dynamics of temperature variations are in order of minutes and the consumed power as an auxiliary component are neglected. The thermal system as shown in Figure 6 consists of a working cooling fluid, a pump, a radiator and a fan. In this work, the control parameter to adjust the stack temperature is the pump mass flow rate. The bond graph implementation is shown in Figure 7.

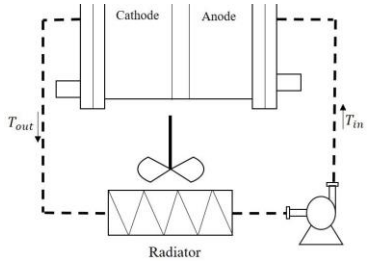

Figure 6 : Cooling system section schematic

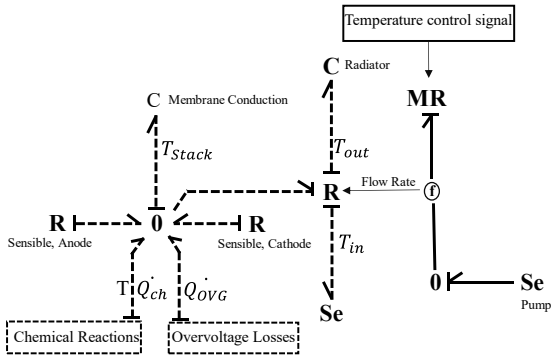

Figure 7 : Bond graph implementation of the thermal management

The produced heat by the chemical reactions $\dot{Q_{ch}}$ and the over voltages $\dot{Q_{ov}}$ and sensible heat $\dot{Q_{sens}}$ are involved in the heat transfer equation of the stack in Equation 14.

$$M_{st} C_{p,st} \frac{dT_{st}}{dt} = -\left(\dot{Q_{ch}} + \dot{Q_{ov}} + \dot{Q_{sens}}\right) \qquad 14$$

The sensible heat of the anode $\dot{Q_a}$, the cathode $\dot{Q_c}$ and the cooling system $\dot{Q_{cs}}$ are determined by Equation 15.

$$\dot{Q_{sens}} = \dot{Q_a} + \dot{Q_c} + \dot{Q_{cs}} \qquad 15$$

The cooling system performance to reduce the stack temperature is dependent on the pump mass flow rate $\dot{m_W}$ for circulating. The thermal relation for the cooling water is expressed as Equation 16. In this work, the outlet temperatures T_{out} of the cooling system is considered constant. It means the only control parameter for the stack temperature is the pump mass flow rate.

$$\dot{Q_{sens,W}} = \dot{m_W} C_{P,W} (T_{out} - T_{in}) \qquad 16$$

The outlet temperature is determined by Equation 17 with logarithmic mean temperature difference. The thermal parameters are from reference (Vasu and Tangirala 2008).

$$T_{out} = T_{st} - exp\left(ln(T_{st} - T_{in}) - \frac{h_w A_W}{\dot{m_W} C_{p,w}} \right) \qquad 17$$

3.5 Hydrogen storage and regulator modelling

The high pressure hydrogen tank and the regulator is simplified due to their fast responses to the actuated signals. The hydrogen storage is considered ideal source with adjustable pressure, which is tuned by a signal from cathode pressure as shown in Figure 8.

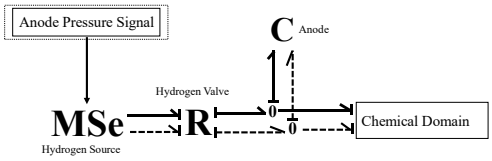

Figure 8 : Schematic of the hydrogen supply sub-system by the bond graph

The model is implemented in 20 sim as a bond graph solver.

4 RESULTS AND DISCUSSION

In the first step, the polarization curve is validated with the reference (Pukrushpan, Stefanopoulou et al. 2004) as is shown in Figure 9. The polarization curve demonstrates the voltage regarding the applied load. The cathode air pressure affects the polarization curve significantly. Because the higher partial oxygen pressure reduces the over voltages. Hence, adjusting the cathode pressure by considering the compressor efficiency obtains the optimum operation point of the system.

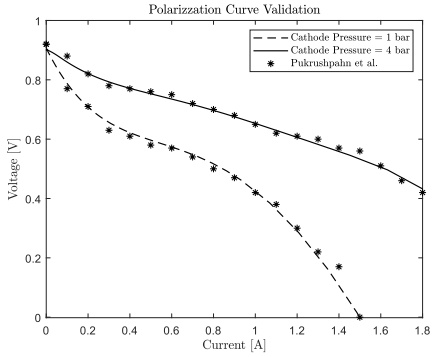

Figure 9: Polarization curve with two cathode operating pressures

In the second step, the voltage transient responses have been compared with (Pukrushpan, Stefanopoulou et al. 2004) by the same load and the compressor voltage. There is acceptable agreement among the obtained results and the reference. The voltage responses, the load and the compressor voltage signals are shown in Figure 10.

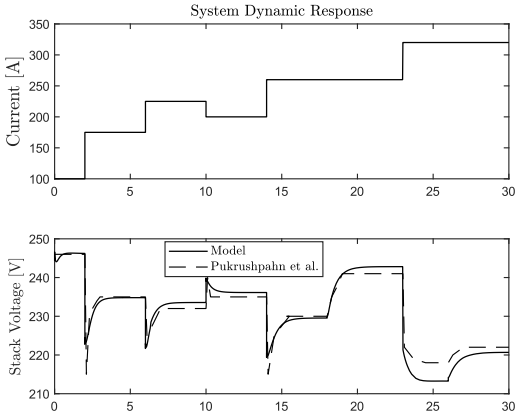

Figure 10: The voltage dynamic responses regarding the applied loads and the compressor voltage signals

In Figure 10, the compressor voltage signals follow load steps until t=15 s. Therefore, as it is shown in Figure 11 the oxygen excess ratio defined as the consumed oxygen to the supplied oxygen which is maintained constant. At t=18 s there is step in the compressor signal voltage but no changes in the load. Thus, the oxygen partial pressure increased due to mass accumulation in the cathode. Moreover, at t=24s the step load is applied but no voltage signal to the compressor, as a result the oxygen pressure decreased. In Figure 11from t=18 s to t=26 s the compressor mass flow rate is constant but there is variations in the oxygen partial pressure due to accumulated mass in the cathode, which shows the importance of the partial pressure calculations in the cathode.

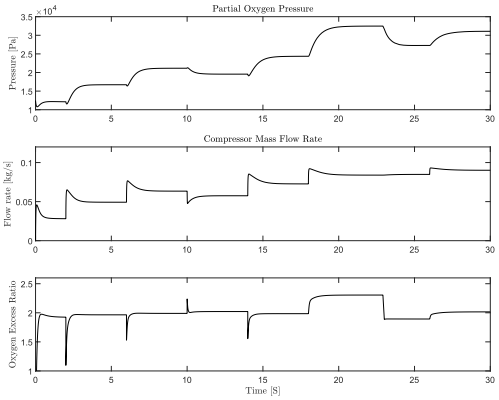

Figure 11: Air supply system performance, partial oxygen pressure is calculated based on the compressor mass flow rate and the consumption, the oxygen excess ratio shows oxygen consumption to the supplied

The over voltage behaviours regarding the applied loads are shown in Figure 12. The activation loss depends on the partial oxygen pressure. Hence, during the load increment the partial oxygen pressure is increased. As result, the activation loss is decreased. The ohmic over voltage has linear behaviour to the current and less dependency to the partial oxygen pressure. However, the ohmic loss is affected by the humidity and in this work the humidity of the membrane is considered ideal and 100%. Hence, there is no significant variations to the ohmic loss. The concentration over voltage is predominant in the high current densities and even in low loads it can be neglected. Also, operation in the high current loads is avoided in the real cases due to less efficiency.

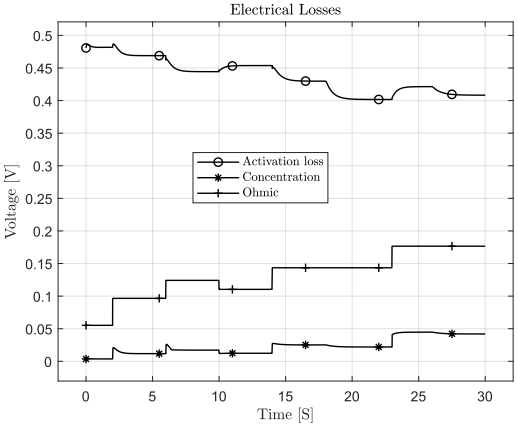

Figure 12: Electrical losses with the applied load for the dynamic validation

System efficiency and the stack efficiency are shown in Figure 13. There is a considerable difference between these two parameter. The compressor as an auxiliary component consumes part of the produced power by the stack. So, part of the produced power is dedicated to the air supply system to provide the stack condition for the main power producing. The system efficiency is the performance that is expected from a PEMFC system as power source in power systems. There is a significant discrepancy in the low current due to constant initial power consumption by the compressor and the low produced power by the stack. In the higher current the produced power by the stack increases and this discrepancy decreases. In the efficiency calculations of the fuel cells the power consumption by the auxiliary components should be considered.

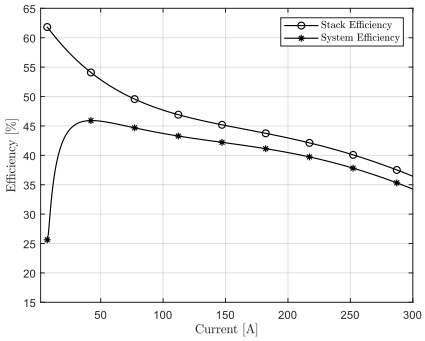

Figure 13: Comparison of the system efficiency and the net efficiency

5 CONCLUSION

In this work, the model of the PEMFC system by the bond graph method is presented with real time capabilities.

The main emphasis was on the modeling of auxiliary systems and connections besides the stack modelling. Because the PEMFC system performance is dependent on the sub-systems. Hence, the system is divided into four sections as the air supply, the hydrogen supply, the stack and the thermal management. The electrochemical reactions in the stack are modelled by empirical

relations. However, the sub-systems and the gas dynamics in the stack are modelled based on physics. The air supply system is more complex than the hydrogen supply system because of the compressor and the manifolds. The air supply affects the PEMFC system from a system efficiency and dynamic responses point of view.

The bond graph approach proposes a modular and flexible strategy for modelling multi disciplinary systems. Each section or sub-system can be modelled individually and connected through power conversion bonds to other sub-systems, which is practical in multi physics systems. For instance, in this model the air supply system begins with a voltage signal to produce torque in the compressor until partial pressure calculations in the cathode. Afterward, it is connected to the electochemical section by the pseudo bonds. It contains various physics, which are implemented and also represented graphically. In addition, the less computational time facilities utilizing the model in simulators and design optimization problems.

The system efficiency is compared with the stack efficiency, which shows the effect of auxiliary systems on the PEMFC performance. Moreover, dependency of the voltage dynamics is discussed regarding the compressor signals and the partial oxygen pressure. Since, in hybrid power systems, the PEMFC system efficiency and dynamic responses are important parameters to be considered. In the end, the model can be utilized for simulator applications with real time capabilities and various configurations of the auxiliary systems due to the modular approach of the bond graph.

ACKNOWLEDGMENTS

This work is funded by The Research Council of Norway, SFI Smart Maritime with project code 237917.

REFERENCES

Benchouia, N. E., et al. (2014). "Bond graph modeling approach development for fuel cell PEMFC systems." International journal of hydrogen energy **39**(27): 15224-15231.

Chu, D., et al. (2000). "Analysis of PEM fuel cell stacks using an empirical current–voltage equation." Journal of Applied Electrochemistry **30**(3): 365-370.

Dawes, J., et al. (2009). "Three-dimensional CFD modelling of PEM fuel cells: an investigation into the effects of water flooding." Chemical Engineering Science **64**(12): 2781-2794.

Karnopp, D. (1978). "Pseudo bond graphs for thermal energy transport."

Pedersen, E. (2001). "Modelling multicomponent two-phase thermodynamic systems using pseudo-bond graphs." SIMULATION SERIES **33**(1): 257-263.

Pukrushpan, J. T., et al. (2004). "Control-oriented modeling and analysis for automotive fuel cell systems." J. Dyn. Sys., Meas., Control **126**(1): 14-25.

Pukrushpan, J. T., et al. (2004). Control of fuel cell power systems: principles, modeling, analysis and feedback design, Springer Science & Business Media.

Vasilyev, A., et al. (2017). "Component-based modelling of PEM fuel cells with bond graphs." International journal of hydrogen energy **42**(49): 29406-29421.

Vasu, G. and A. Tangirala (2008). "Control-orientated thermal model for proton-exchange membrane fuel cell systems." Journal of Power Sources **183**(1): 98-108.

Vijay, P., et al. (2009). "A bond graph model-based evaluation of a control scheme to improve the dynamic performance of a solid oxide fuel cell." Mechatronics **19**(4): 489-502.

AUTHOR BIOGRAPHIES

KAMYAR MALEKI BAGHERABADI received B.Sc. of mechanical engineering-applied design from Iran University of Science and Technology in 2014 and M.Sc. of mechanical engineering-energy conversion in 2016 from Sharif University of Technology. He is PhD candidate in marine department of Norwegian University of Science and Technology since 2019. His background is mostly on simulation and numerical modelling in various fields from solid mechanics, multibody dynamics, fluid mechanics, electro-chemicals fluid flow and CFD. His current research interests are system modelling of marine power plants with fuel cells for the aim of cosimulation and size optimization. His email address is kamyar.maleki@ntnu.no.

STIAN SKJONG received the M.Sc. degree in 2014 and the Ph.D. degree in 2017, both in marine technology from the Norwegian University of Science and Technology(NTNU), Ålesund,Norway. He is currently working as a Research Scientist with SINTEF Ocean, Trondheim, Norway. His research interests include modeling, simulation and control of marine systems, nonlinear control, model-based control designs, cosimulation strategies for virtual prototyping of marine systems and operations, and simulation software development. His email address is Stian.Skjong@sintef.no.

EILIF PEDERSEN received the M.Sc. degree in Marine Engineering from the Norwegian Institute of Technology, Norway, in 1983. He has been with the Norwegian Marine Technology Research Institute, as a Senior Research Engineer until 1999, where he joined the NTNU as an Associate Professor. He has held multiple positions, such as a Vice Dean of Education with the Faculty of Engineering Science and Technology, the Head of Master Programs in marine technology, the Leader with the Research Group of Marine Systems, and the Head of Machinery Laboratory at the Department of Marine Technology. His areas of expertise are in the field of modeling methodology and simulation of dynamic multidisciplinary and mechatronic systems focusing on machinery system dynamics, internal combustion engines, vibrations, thermal- and hydraulic machines, fuel cell system dynamics, and hybrid power plants for marine applications. His email address is Eilif.pedersen@ntnu.no.